ELSEVIER

Physica C 352 (2001) 67–72

PHYSICA C

www.elsevier.nl/locate/physc

Transport properties of normal and ferromagnetic atomic-size constrictions with superconducting electrodes

A. Martín-Rodero [a,*], A. Levy Yeyati [a], J.C. Cuevas [b]

[a] *Departamento de Física Teórica de la Materia Condensada C-V, Facultad de Ciencias, Universidad Autónoma de Madrid, E-28049 Madrid, Spain*

[b] *Institut für Theoretische Festkörperphysik, Universität Karlsruhe 76128 Karlsruhe, Germany*

Abstract

We present a theoretical approach to the transport properties of normal (N) and ferromagnetic (F) atomic-size contacts between superconducting (S) electrodes. This approach is based on non-equilibrium Green function techniques and a Hamiltonian description of the electron transfer processes in the constriction region. For a normal atomic-size contact the theory allows to relate the conduction channels to the atomic orbital structure. In the ferromagnetic case spin polarization gives rise to a spin dependent transmission distribution. For the case of S–N–S constrictions this theory predicts a d.c. current and shot noise in remarkable agreement with recent experimental results. We also analyze S–F and S–F–S constrictions. In this last case the current–voltage characteristic exhibits a very peculiar subgap structure associated to the competition between the multiple Andreev reflection mechanism and the ferromagnetic spin polarization. © 2001 Elsevier Science B.V. All rights reserved.

Keywords: Mesoscopic superconductivity; Ferromagnetism; Quantum point contacts; Subgap structure

1. Introduction

Recent experimental techniques have made possible the fabrication of mesoscopic structures on the nanometer scale. The use of scanning tunneling microscopy an mechanically controllable break junction techniques [1], has allowed to obtain atomic-size constrictions of different metallic elements in a rather reproducible way. The fact that a conductor of atomic cross section can only accommodate a small number of conduction channels [2] has made possible a quantitative comparison between theory and experiments [3–5]. The agreement is so remarkable as to provide detailed information about the quantum channel distribution of the contact.

On the theoretical side, much progress has been achieved with the development of fully quantum mechanical theories for the a.c. Josephson effect in the S–N–S case [6–8]. Two basically different approaches have been used: a phenomenological scattering approach [6,9] based on matching solutions of the time dependent Bogoliubov-de Gennes equations with appropriate boundary conditions; and a more microscopical approach based on model Hamiltonians [7,10,11]. Both approaches have been shown to give equivalent results under certain simplifying assumptions [7]. Although the scattering approach may be somewhat

* Corresponding author. Fax: +34-91-397-4950.

E-mail address: alvaro@uamca1.fmc.uam.es (A. Martín-Rodero).

0921-4534/01/$ - see front matter
PII: S0921-4534(00)01679-8

simpler, the Hamiltonian approach have certain advantages in dealing with situations where self-consistency effects are important [10] or when electron correlation effects are important [11]. Among the predictions of the microscopic theory for S–N–S contacts one can mention the subgap structure on the d.c. current which is in quantitative agreement with the experimental results [2,4] and the enhancement of shot noise at small bias voltage [12,13].

On the other hand there is a growing interest in the study of electronic transport in mesoscopic systems containing ferromagnetic parts. One would expect novel phenomena due to the broken spin symmetry which gives rise to spin dependent transport. The possibility of controlling the current by the application of magnetic fields has been recently pointed out [14]. Moreover the electronic transport in nanometric systems containing superconductor/ferromagnet interfaces presents the additional interest of exhibiting the competing mechanisms of Andreev reflection and spin polarization.

In Section 2, we present a microscopic theory of electron transport through normal and ferromagnetic atomic contacts. The energy dependent transmission of the contact is calculated using an atomic orbital basis. Section 3 is devoted to a brief review of the theory of a superconducting contact. In Section 4 the conduction properties of a S–F contact are analyzed and an explicit expression of the Andreev conductance is obtained. Finally Section 5 is devoted to discuss the d.c. transport properties of a S–F–S contact showing how the competition of multiple Andreev reflections (MAR) and spin polarization dramatically modify the subharmonic gap structure with respect to the S–N–S case.

2. Normal and ferromagnetic atomic constrictions

An idealized geometry for a one-atom contact is depicted in Fig. 1. It consists of two fcc pyramids connected to a central atom. The layers in this structure are labeled from 1 to N and are connected to perfect semi-infinite fcc crystals. As we are considering metallic systems of atomic dimensions a natural choice of basis set is one formed by atomic orbital functions. Written in terms of an atomic orbital basis the electronic Hamiltonian of the system adopts the usual tight-binding form

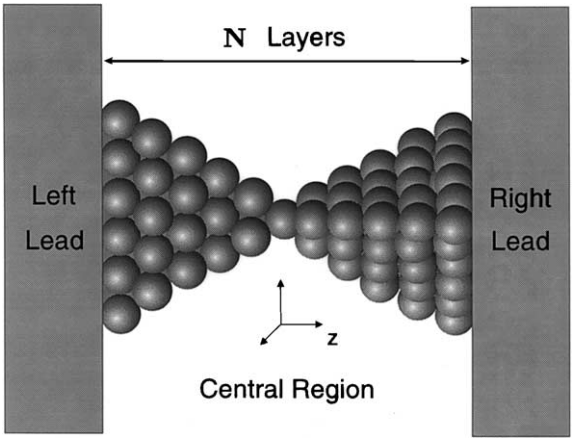

Fig. 1. Idealized model geometry for a one-atom contact.

$$\hat{H} = \sum_{i\alpha,\sigma} \epsilon_{i\alpha} c^{\dagger}_{i\alpha\sigma} c_{i\alpha\sigma} + \sum_{i\alpha \neq j\beta,\sigma} t_{i\alpha,j\beta} c^{\dagger}_{i\alpha\sigma} c_{j\beta\sigma}, \tag{1}$$

where i, j runs over the constriction atomic sites and α, β denote the different atomic orbitals. The hopping elements $t_{i\alpha,j\beta}$ are assumed to connect first-neighboring sites. For the determination of the tight-binding parameters of Eq. (1) we follow the parameterization given in Ref. [15] which is known to reproduce accurately the electronic bulk properties for different metallic elements. For the present calculation only those atomic orbitals having a significant contribution to the electronic density of states (DOS) at the Fermi energy, E_F, will be taken into account. One important ingredient in an analysis of the electronic properties of a metallic system is the fulfillment, at least in an approximate way, of local charge neutrality. This can be achieved within our model by a self-consistent variation of the diagonal levels $\epsilon_{i\alpha}$.

The transport properties of this model can be straightforwardly obtained using standard Green function techniques [3]. The current through the constriction can be written in a Landauer form as

$$I = \frac{2e}{h} \int_{-\infty}^{\infty} T(E,V)[f_L(E) - f_R(E)]\mathrm{d}E, \tag{2}$$

where $f_{L,R}$ are the Fermi distribution functions for the (left, right) leads and $T(E,V)$ is the transmission which can be written in terms of the system Green functions as

$$T(E,V) = 4\mathrm{Tr}\left[\hat{\Gamma}_L(E)\hat{G}^r_{1N}(E)\hat{\Gamma}_R(E)\hat{G}^a_{N1}(E)\right].$$

In this expression $\hat{G}^r_{1N}$ and $\hat{G}^a_{N1}$ are matrices whose elements are the Green functions connecting layers 1 and N, $\hat{\Gamma}_{L,R}$ being matrix tunneling rates describing the coupling of the central region to the leads (see Ref. [3] for additional details).

The current is thus expressed in terms of a transmission matrix, the diagonalization of which allows to write the conductance as a superposition of independent conduction channels

$$G = \frac{2e^2}{h}\sum_i T_i. \tag{3}$$

The results of this model allow to correlate the number of conducting channels of an atomic contact with the number or atomic orbitals giving a contribution to the contact DOS at the Fermi level which roughly corresponds to the number of valence electrons in the atom. For a one atom contact this theory thus predicts a single conduction channel for simple metals like Au and Ag, three channels for sp-like metals like Al and Pb up to five for a transition metal like Nb. The number of conducting channels as well as the individual values of the transmissions are in good agreement with the experimental results [4].

Let us now analyze the transport properties of ferromagnetic atomic contacts. In this case, the diagonal and non-diagonal matrix elements in Hamiltonian (1) will in general become spin dependent. As in the case of normal metallic contacts, we follow the parameterization given in Ref. [15]. Although an accurate calculation would require the self-consistent determination of both charge and magnetization at each site in the contact geometry, for a qualitative analysis we will use the unmodified bulk parameters.

As an illustration in Fig. 2 we present calculations of the spin dependent transmission of a Co atomic contact. As can be observed there is a large difference in the total transmission at the Fermi energy, which is close to three for spin down and ~0.5 for spin up. A more detailed analysis reveals that the total conductance is due to the contribution of up to six conduction channels. While the down spin channels have mainly a d character the up spin ones are dominated by the s orbitals (details on the calculation will be given elsewhere).

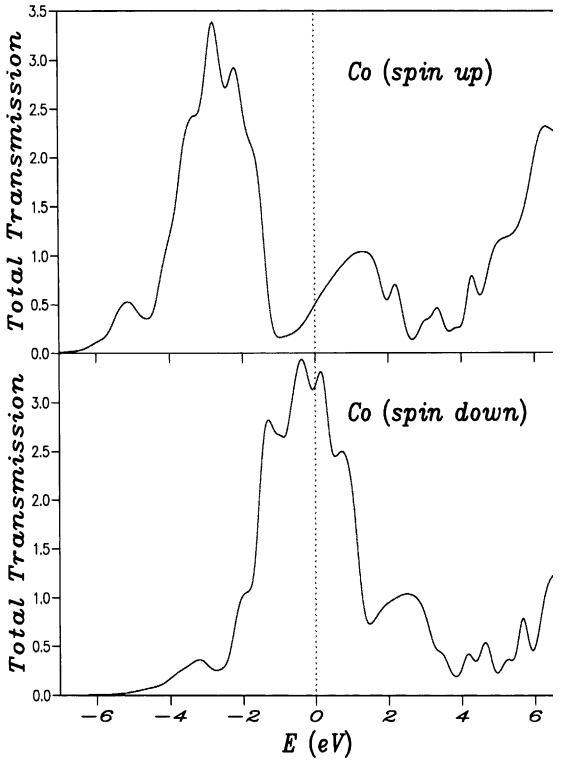

Fig. 2. Calculated total spin-dependent transmission for a Co one-atom contact using parameters of Ref. [15].

3. Fully quantum mechanical theory of a superconducting contact

In Section 2 it was shown that the normal transport properties of the contact can be described as a superposition of a few independent conduction channels. In the superconducting case it can be shown that this superposition is still valid [16]. This fact permits to concentrate in obtaining a fully quantum mechanical solution for the single channel case.

Within the same spirit of the model discussed in Section 2 we may use the following time-dependent Hamiltonian for analyzing a one channel superconducting contact

$$\hat{H}(\tau) = \hat{H}_{\mathrm{L}} + \hat{H}_{\mathrm{R}} + \sum_{\sigma} \left(t \mathrm{e}^{\mathrm{i}\phi(\tau)/2} c^{\dagger}_{\mathrm{L}\sigma} c_{\mathrm{R}\sigma} + t^{*} \mathrm{e}^{-\mathrm{i}\phi(\tau)/2} c^{\dagger}_{\mathrm{R}\sigma} c_{\mathrm{L}\sigma} \right), \tag{4}$$

where $\hat{H}_{\mathrm{L}}$ and $\hat{H}_{\mathrm{R}}$ correspond to the uncoupled electrodes while the hopping term describes the electron transfer processes between the outermost sites on both electrodes. The normal transmission coefficient T of the contact adopts a simple expression as a function of t, $T = 4(t/W)^2/[1+(t/W)^2]^2$, where $W = 1/\pi\rho_{\mathrm{F}}$, ρ_{F} being the normal DOS at the Fermi energy on both electrodes. In this model the time dependence appears through the phase difference $\phi(\tau)$, which for constant bias voltage is equal to $2eV\tau/\hbar$.

The transport properties can be calculated using non equilibrium Keldysh Green function techniques [17]. In Ref. [7] the a.c. and d.c. components of the current are calculated under a constant applied voltage. It is worth noticing that the calculated $I(V)$ curves have provided an accurate fitting of the experimental results, which has made it possible to extract the channel content of an atomic contact [2]. This information is in agreement with the predictions of the atomic orbital calculation discussed in Section 2.

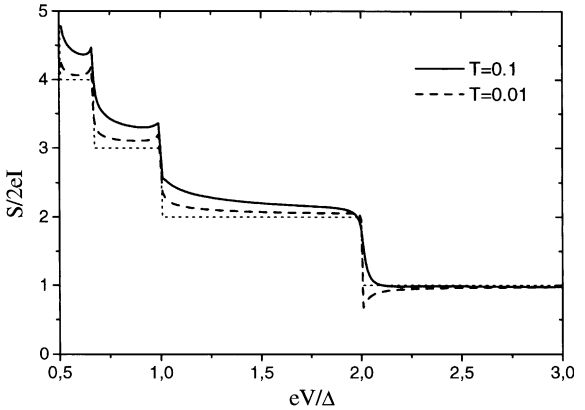

Fig. 3. Effective charge defined as $Q^{*} = S/2eI$ in the low transmission regime for a one-channel superconducting contact.

We have also studied thermal and shot noise using this model in Refs. [12,18]. In the case of shot noise one of the most remarkable predictions is the appearance for low transmission of well defined plateaus at integer values in the effective charge defined as $Q^{*} = S(V)/2eI$ as shown in Fig. 3. Preliminary experimental results seem to confirm this prediction [19].

4. The F–S contact

Let us now consider a contact formed by a superconductor and a ferromagnetic electrode. An atomic size contact of this type could be feasible using for instance the STM technique with a superconducting tip and a ferromagnetic substrate. As a first step we will concentrate here on a single mode contact. In a model such as the one described in Section 3 one can take into account the effect of spin polarization in the transmission coefficients by introducing a spin dependent hopping amplitude ($t_{\uparrow}$ and $t_{\downarrow}$) in the term coupling both electrodes. In this way one obtains the following expression for the spin dependent transmission

$$T_{\sigma} = 4(t_{\sigma}/W)^2/[1 + (t_{\sigma}/W)^2]^2. \tag{5}$$

This modelization is equivalent to one in which the spin polarization is introduced in the ferromagnetic electrode DOS.

In the N–S contact with no spin polarization whatsoever the Andreev conductance ($eV < \Delta$) can be written as [7,20]

$$G_{\mathrm{NS}}(V) = \frac{4e^2}{h} \frac{T^2}{(1+R)^2 - 4R^2(eV/\Delta)^2}, \tag{6}$$

where $R = 1 - T$ is the reflection probability. It would seem reasonable that a similar expression will hold in the S–F case with T, R substituted by some effective values T_{eff}, R_{eff}. In fact, it turns out that the correct expression for $G_{\mathrm{FS}}(V)$ is identical to that of Eq. (6) with T, R substituted by their mean geometrical averages $\bar{T} = \sqrt{T_{\uparrow}T_{\downarrow}}$ and $\bar{R} = \sqrt{R_{\uparrow}R_{\downarrow}}$:

$$G_{\mathrm{FS}}(V) = \frac{4e^2}{h} \frac{\bar{T}^2}{(1+\bar{R})^2 - 4\bar{R}^2(eV/\Delta)^2}. \tag{7}$$

In Fig. 4 it is shown the F–S conductance as a function of voltage for different values of the spin dependent transmissions. As it is evident from Eq. (7), for perfect transmission in one of the spin channels, $\bar{R} = 0$, and $G_{FS}(V)$ is constant in the subgap region. On the other hand, for a generic situation the conductance exhibits the usual double peaked structure at $eV = \pm\Delta$ although reduced with respect to the universal value $4e^2/h$ found in the N–S case, by a factor $\bar{T}^2/(1-\bar{R})^2$.

For describing a more realistic F–S contact, one should take into account the presence of several conducting channels (see Section 2), even for a one-atom contact. One should mention that the analysis of the multichannel situation is in this case more involved than in the N–S case due to the broken spin symmetry which makes the hypothesis of superposition of channels not strictly valid [16].

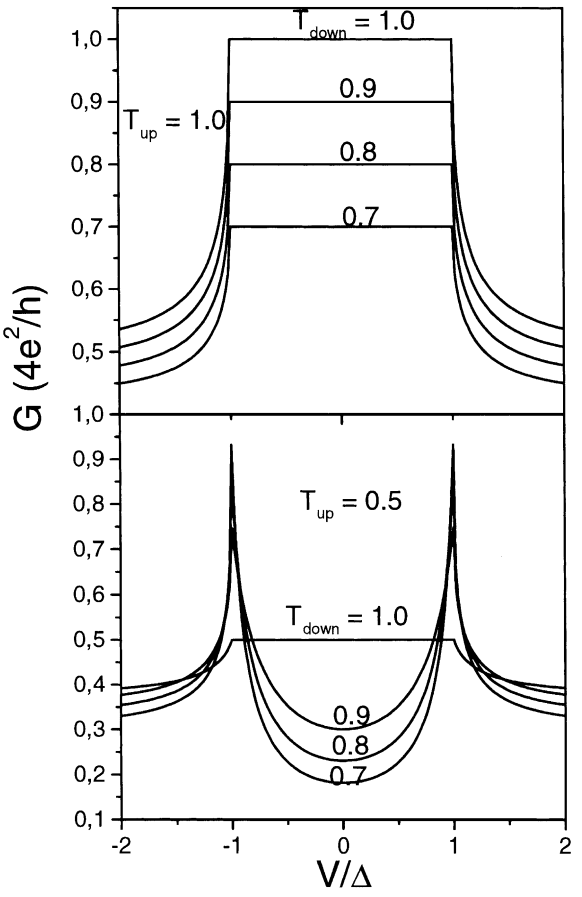

Fig. 4. Differential conductance for a F–S contact for different values of the spin-dependent transmissions.

5. S–F–S contacts

We shall consider in this section a situation in which a small ferromagnetic region is placed between two superconducting electrodes. This could be achieved by depositing a ferromagnetic metal layer over a superconducting substrate using a superconducting STM tip as a second electrode. We assume that the width of the ferromagnetic layer is much smaller than the superconducting coherence length.

The S–N–S case can be straightforwardly generalized to the present situation by the inclusion of a spin dependent transmission across the ferromagnetic region, T_σ, as discussed in Section 4.

One would expect the appearance of interesting effects due to the interplay between spin-polarization and MAR. In fact, the subgap structure (SGS) in the $I(V)$ curves is dramatically affected by the presence of spin polarization. For the sake of simplicity we shall concentrate here on the case with $T_\uparrow \sim 1$ and study the SGS for decreasing values of $T_\downarrow$. For comparison the $I(V)$ curves for the non-magnetic case are also shown. The corresponding $I(V)$ curves are depicted in Fig. 5. As can be observed, as $T_\downarrow$ is decreased, an increasingly pronounced structure begins to develop at certain subgap energies. Surprisingly these energies do not correspond to integer fractions of 2Δ as in the S–N–S case. For low values of $T_\downarrow$ the resonances in the $I(V)$ curves appear to be located at $eV = \Delta/(\sqrt{2}n)$. This striking behavior can be explained as follows. In the present case with a spin dependent transmission coefficient, the position of the Andreev bound state levels can be shown to be given by the following expression:

$$\epsilon(\phi) = \pm\frac{\Delta}{\sqrt{2}}\sqrt{1+\bar{R}+\bar{T}\cos(\phi)}. \tag{8}$$

Thus, when $T_\uparrow \sim 1$ and $T_\downarrow \to 0$ the bound states become progressively localized at $\epsilon(\phi) = \pm\Delta/\sqrt{2}$. When a bias voltage is applied, MAR can connect the resonances in the spectral density corresponding

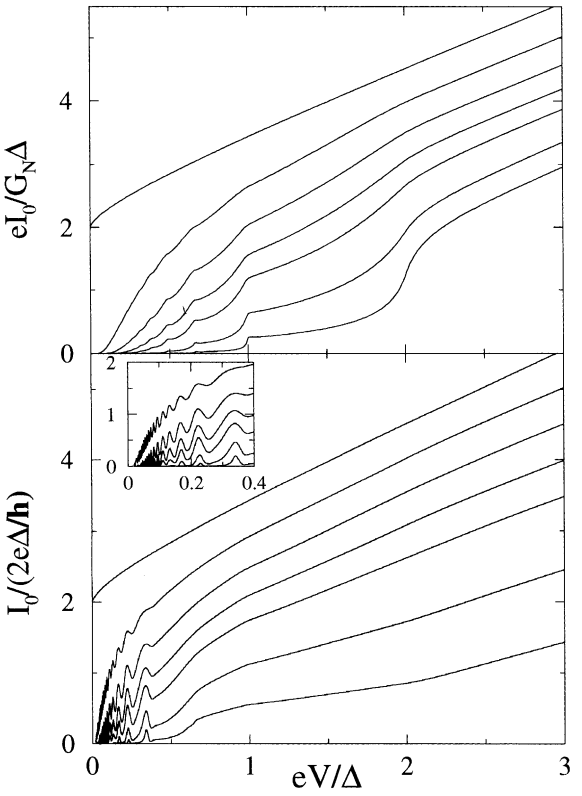

Fig. 5. d.c. Current–voltage characteristic for a S–F–S contact. (a) non-magnetic case ($T_\uparrow = T_\downarrow$) and (b) $T_\uparrow = 1.0$ and decreasing values of $T_\downarrow$: 1.0, 0.9, 0.8, 0.7, 0.6, 0.4, 0.2. The inset shows an enlarged view of the low bias region.

to these bound states giving current peaks at the condition $eV = \Delta/(\sqrt{2n})$.

6. Conclusions

In conclusion we have presented a theoretical approach to study the transport properties of atomic size contacts including superconducting and ferromagnetic parts. For normal and superconducting contacts the predictions of the theory are in quantitative agreement with existing experimental data. The inclusion of ferromagnetic parts produces a spin dependent transmission. The interplay of spin polarization and Andreev reflection gives rise to interesting features, in particular, to novel subgap structure in the superconducting d.c.

Acknowledgements

This work has been supported by the Spanish CICYT under contract no. PB97-0044 and by the SFB 195 of the German Science Foundation.

References

[1] J.M. van Ruitenbeek, in: L.L. Sohn, L.P. Kouwenhoven, G. Schön (Eds.), Mesoscopic Electron Transport, NATO-ASI Series E: Appl. Sci., vol. 345, Kluwer Academic Publishers, Dordrecht, 1997, p. 549.
[2] E. Scheer, et al., Phys. Rev. Lett. 78 (1997) 3535.
[3] J.C. Cuevas, A.L. Yeyati, A. Martín-Rodero, Phys. Rev. Lett. 80 (1998) 1066.
[4] E. Scheer, et al., Nature (London) 394 (1998) 154.
[5] J.C. Cuevas, et al., Phys. Rev. Lett. 81 (1998) 2990.
[6] D. Averin, A. Bardas, Phys. Rev. Lett. 75 (1995) 1831.
[7] J.C. Cuevas, A. Martín-Rodero, A.L. Yeyati, Phys. Rev. B 54 (1996) 7366.
[8] E.N. Bratus, et al., Phys. Rev. B 55 (1997) 1266.
[9] E.N. Bratus, V.S. Shumeiko, G. Wendin, Phys. Rev. Lett. 74 (1995) 2110.
[10] A. Martín-Rodero, F.J. García-Vidal, A.L. Yeyati, Phys. Rev. Lett. 72 (1994) 554.
[11] A.L. Yeyati, J.C. Cuevas, A. López-Dávalos, A. Martín-Rodero, Phys. Rev. B 55 (1997) R6137.
[12] J.C. Cuevas, A. Martín-Rodero, A.L. Yeyati, Phys. Rev. Lett. 82 (1999) 4086.
[13] Y. Naveh, D.V. Averin, Phys. Rev. Lett. 82 (1999) 4090.
[14] H. Oshimay, K. Miyano, Appl. Phys. Lett. 73 (1998) 2203.
[15] D.A. Papaconstantopoulous, Handbook of the Band Structure of Elemental Solids, Plenum Press, New York, 1986.
[16] C.W.J. Beenakker, Phys. Rev. B 46 (1992) 12841.
[17] L.V. Keldysh, Sov. Phys. JETP 20 (1965) 1018.
[18] A. Martín-Rodero, A.L. Yeyati, F.J. Garcia-Vidal, Phys. Rev. B 53 (1996) R8891.
[19] C. Urbina, private communication.
[20] G.E. Blonder, M. Tinkham, T.M. Klapwijk, Phys. Rev. B 25 (1982) 4515.